Magnetism and energetics of Mn-Doped ZnO ($10\bar{1}0$) thin films

Q. Wang, Q. Sun, B. K. Rao, and P. Jena

Physics Department, Virginia Commonwealth University, Richmond, Virginia 23284, USA

First-principles calculations based on gradient corrected density functional theory are performed on Mn-doped ZnO thin film. Magnetism and energetics are studied for two Mn concentrations and varying Mn configurations. It is found that in the dilute limit when Mn atoms are far apart, the ferro-magnetic and antiferromagnetic states are energetically nearly degenerate. The resulting fluctuation would, therefore, make the system paramagnetic as found in the experiment. But, as the concentration of Mn atoms increases, there is a tendency for Mn atoms to form nearest neighbors and cluster around oxygen. For such a configuration, the antiferromagnetic coupling between Mn atoms is energetically more favorable. The results are compared with a diverse range of experiments on Mn-doped ZnO thin film.

　　　　PACS number(s): 75.50.Pp, 71.55.−i, 61.72.Ss, 71.15.Nc

There is considerable current interest in exploiting electron spin in the design and synthesis of novel spin-based electronic materials. In this context, the discovery of ferromagnetism in (Ga, Mn)As (Ref. 1) with a Curie temperature (T_c) of 110 K and subsequent theoretical prediction[2] that T_c could exceed room temperature in (Ga, Mn)N and (Zn, Mn)O have created considerable theoretical and experimental interest in dilute magnetic semiconductor (DMS) systems. The doping of Mn in GaN and ZnO has many attractive features. The large energy gap of 8.4 eV between the filled $4s$ and half filled $3d$ valence orbitals of Mn prevents their significant hybridization in bulk environment. Consequently, the chemistry of the Mn atom is governed by its $4s^2$ electrons, while its magnetic properties are determined by the $3d^5$ shell. No other transition metal shows this dichotomy of behavior. Thus, doping of Mn, which is expected to carry large magnetic moments, brings a new functionality to these DMS materials.

While much of the past work has concentrated on (Ga, Mn)N systems,[3] it is only recently that attention has been focused on Mn doped ZnO.[4–6] Compared to other wide-band gap materials, ZnO has a higher exciton binding energy of 60 meV,[7] and ZnO-based DMS's are transparent to visible light.[8] This makes ZnO thin film one of the most promising materials for fabricating ultraviolet light-emitting and laser devices as well as new devices making use of magneto-optical effects. Therefore, ZnO thin film has become a hotly pursued system.[9–17] However, experiments give puzzling results concerning the magnetism and structure. For example, Jung *et al.* and Sharma *et al.*[4] reported that ferromagnetism appears in Mn-doped ZnO thin film, while Ueda *et al.*[12] found that no ferromagnetism exists in Mn-doped ZnO thin film prepared by using a pulsed-laser deposition technique. Furthermore, Fukumura *et al.* found that a strong antiferromagnetic coupling exists in this system.[17] Similarly while homogeneous distribution of Mn in epitaxial ZnO thin films was reported by Cheng *et al.*,[6] clustering of Mn atoms in ZnO thin film is reported by Jin *et al.* in recent experiments.[10] To understand these puzzling observations and to clarify the magnetic properties and structure of this technologically important Mn-doped ZnO film, theoretical studies are highly desirable.

The central questions are as follows. (1) In what way is doping of Mn into ZnO different from that into GaN? (2) Is it energetically favorable to replace a Zn site with Mn and if so do the Mn atoms prefer to occupy the surface or subsurface sites? (3) As the concentration of Mn increases, do the Mn atoms prefer to cluster in ZnO as they do in GaN? (4) Is the coupling between Mn atoms in ZnO thin film ferromagnetic or antiferromagnetic and what is the difference in their energies? (5) How does the concentration of Mn affect the magnetic properties of (Zn, Mn)O?

In this paper we address some of the above questions. We do this by calculating the total energies, electronic structure, and magnetic properties of Mn-doped ZnO ($10\bar{1}0$) thin film for two different Mn concentrations and for Mn atoms replacing various Zn sites. The calculations were carried out using density functional theory and generalized gradient approximation for exchange and correlation,[18] which has met with considerable success in predicting the properties of Mn and Mn oxide clusters. For example, the magnetic moment of the Mn_{13} cluster predicted by Nayak *et al.*[19] has been recently confirmed by magnetic deflection experiment of Knickelbein.[20] Similarly the prediction of the electron affinity of MnO_4-anion is in quantitative agreement with experiment.[21]

We have modeled the ($10\bar{1}0$) film by a slab of eight layers containing 64 atoms in the supercell. To preserve symmetry, the two top and bottom layers of the slab were taken to be identical, and each slab was separated from the other by a vacuum region of 10 Å. The central four layers were held fixed at their bulk configuration while the surface and subsurface layers on either side of the slab were allowed to relax without any symmetry constraint. Calculations of the total energies and forces, and optimizations of geometry were carried out using a plane-wave basis set with the projector augmented plane wave (PAW) method[22] as implemented in the Vienna *ab initio* Simulation Package (VASP).[23] K-point convergence was achieved with $(6 \times 4 \times 1)$ Monkhorst-Pack[24] grid, and tests with up to $(8 \times 6 \times 2)$ Monkhorst k-point mesh were made. The energy cutoff was set at 350 eV and the convergence in energy and force were 10^{-4} eV and 3×10^{-3} eV/Å, respectively. Tests performed on slabs con-
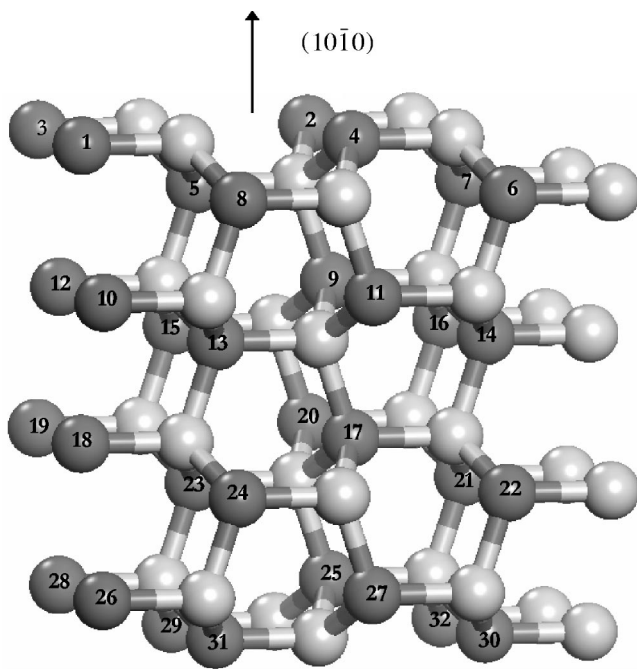
　　　　69 233310-1

FIG. 1. The supercell of ZnO $(10\bar{1}0)$ slab consisting of 32 Zn and 32 O atoms. The numbered atoms are Zn.
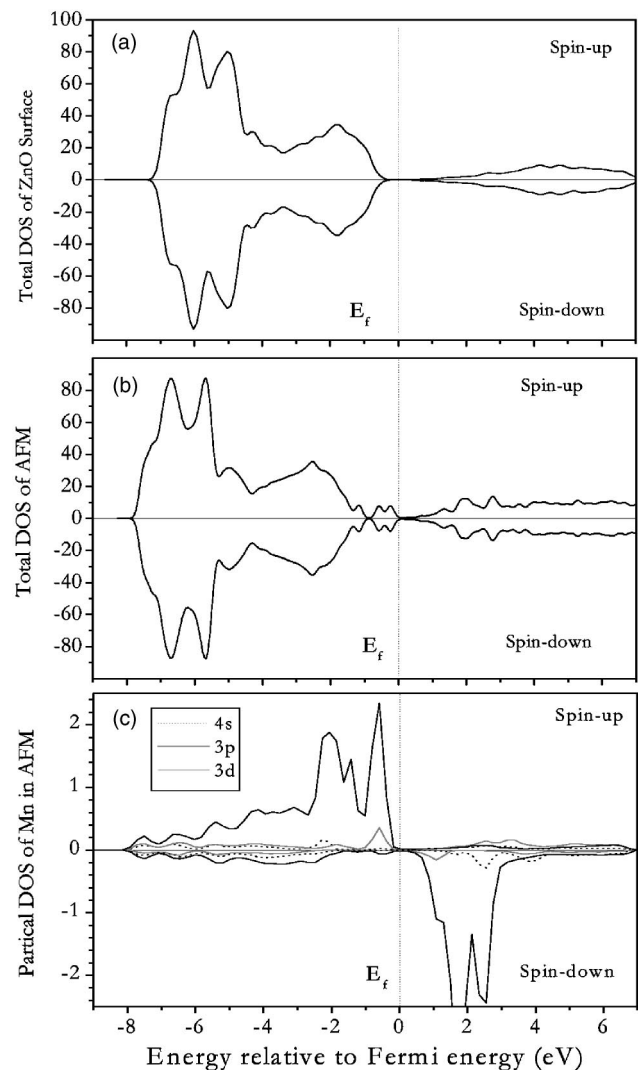

FIG. 2. Total DOS for (a) pure and (b) Mn-doped ZnO thin film in the antiferromagnetic ground state. The corresponding partial DOS of Mn atom is shown in (c).

taining six and ten layers (48 and 80 atom/supercell, respectively) indicated that the results are not sensitive to the number of layers and that a slab composed of eight layers (2 $\times 2$) $(10\bar{1}0)$ wurtzite ZnO is adequate to mimic the surface. In the following we only discuss our results based on the eight-layer slab.

In Fig. 1 we show the supercell containing 32 Zn and 32 O atoms used to represent the $(10\bar{1}0)$ slab. The darker numbered atoms are Zn, and the lighter atoms are O. To compare our results with previous calculations and to assess the sensitivity of our results to slab thickness, we first discuss the surface relaxation and electronic structure of pure ZnO $(10\bar{1}0)$ film. The lateral, vertical, and angular displacements of atoms on the top two layers of the film were calculated. We found that the Zn atom on the surface layer moves outward by 0.28 Å while that on the subsurface layer moves inward by -0.07 Å. Similarly, the Zn-O distance on the surface layer contracts by -6.42% while that on the subsurface layer expands by $+0.4\%$. The relaxations of the atoms in the subsurface layer are an order of magnitude smaller than that in the surface layer. These relaxations have been calculated previously by Wander and Harrison[25] who used a hybrid exchange-correlation functional (B3LYP)[26] and supercells consisting of 8–16 atoms. More recently, Meyer and Marx[27] calculated the relaxations by modeling the surface with slabs consisting of one Zn-O dimer and 4–20 layers containing up to 40 atoms in the supercell. Our results agree well with those calculated by Meyer and Marx[27] in spite of the fact that our supercell contains four Zn-O dimers while that used by Meyer and Marx[27] contains only one Zn-O dimer. The energy gain due to relaxation is calculated by taking the difference between the two slabs before and after relaxation and dividing by the number of surface dimers (which is 4 in our case) that relaxed the most. We find these energies to be about 0.28 eV/dimer. In Fig. 2(a) we plot the total density of states for spin up and down electrons corresponding to pure ZnO $(10\bar{1}0)$ film. Note that the densities of states for spin up and down electrons are identical and hence the film is nonmagnetic.

To study the properties of Mn-doped ZnO, we first have to determine the preferred site of Mn atoms and how these sites change as the concentration of Mn is increased. We discuss the substitution of a *single* Mn atom first. We have considered two different configurations: a surface site (marked No. 4) and a subsurface site (marked No. 5) in Fig. 1. To preserve symmetry, we also had to replace Zn sites on the bottom two layers of the slabs, namely, Nos. 31 and 25, respectively, with Mn. Thus, the supercell consisted of $Zn_{30}Mn_2O_{32}$. This amounts to a Mn concentration of 6.25%. Since the two Mn atoms are too far apart to interact with each other, this supercell geometry can yield information on the properties cor-

responding to dilute Mn substitution. The Mn-O bond on the surface layer was found to contract by -5.17%. Recall that the corresponding Zn-O bond contracted by -6.42%.

The total energy of the slab with Mn occupying the surface site is found to be 0.01 eV lower than when Mn atom occupies the subsurface site. This energy difference is indeed very small, and one can argue that Mn does not exhibit any site preference in ZnO. Thus, at low concentration, Mn could occupy any Zn site in ZnO. This is consistent with the experimental finding[6] that Mn is distributed homogeneously in ZnO in the dilute limit. It is interesting to note that in (Ga, N)Mn thin film, we have found[28] that Mn occupying the surface site lies 1.37 eV below the subsurface site.

In order to study magnetic coupling between Mn atoms, we have replaced *two* Zn sites by *two* Mn atoms on the surface and /or sub-surface locations. Corresponding atoms at the bottom of the slab were also replaced to preserve symmetry. This corresponds to a supercell consisting of $Zn_{28}Mn_4O_{32}$ and a Mn concentration of 12.5%. Once again there are many Zn sites where Mn atoms can be substituted. We have studied eight different configurations. Configuration No. 1 corresponds to the replacement of two nearest-neighbor Zn atoms by Mn on the surface layer marked Nos. 2 and 4 in Fig. 1. Symmetry of the slab then requires that we also replace Zn sites Nos. 29 and 31 with Mn. Configurations 2 and 3 correspond to the replacement of the second-nearest-neighbor and third-nearest-neighbor Zn sites on the surface layer, namely, sites 2, 3, 29, 32 and 1, 2, 30, 29, respectively. Configuration 4 represents the substitution of two nearest Zn sites by Mn with one belonging to the surface and the other to the subsurface plane. This corresponds to Mn atoms substituting sites 2, 5 and 29, 25 in Fig. 1. Configuration 5 corresponds to the substitution of Zn atoms from the surface and subsurface layers forming next-nearest-neighbor position (sites 2, 6 and 29, 27). Configuration 6 is achieved by replacing two nearest-neighbor Zn atoms on subsurface layers by Mn. These correspond to sites 5, 8 and 25, 27 in Fig. 1, and configuration 7 corresponds to the replacement on sites 5, 7 and 25, 28. Finally, configuration 8 represents two furthest Zn atoms on the subsurface layer (sites 5, 6 and 25, 26) replaced by Mn atoms. The distances between two Mn atoms in configurations 1, 2, 3, 4, 5, 6, 7, and 8 are, respectively, 3.25, 5.21, 6.14, 3.22, 5.54, 3.25, 5.21, and 6.14 Å.

The total energies of the $Zn_{28}Mn_4O_{32}$ slab were calculated for all the above eight configurations by allowing Mn atoms to couple ferromagnetically as well as antiferromagnetically. The lowest energy configuration is found to be an antiferromagnetic state where Mn atoms replace the two nearest Zn sites on the surface layer (configuration 1) and are 3.25 Å apart. This suggests that as the concentration of Mn increases, Mn atoms will have a tendency to form clusters around oxygen. This is consistent with the recent experiment[10] in which laser molecular-beam epitaxy method was employed to fabricate epitaxial (Zn,Mn)O thin film in a high throughput fashion, and the local structures were investigated. Mn atoms were found to substitutionally replace Zn atoms in ZnO thin film and to form cluster at high concentration.

In Fig. 3 we plot the relative energies of the ferromagnetic and antiferromagnetic states for all the eight configurations
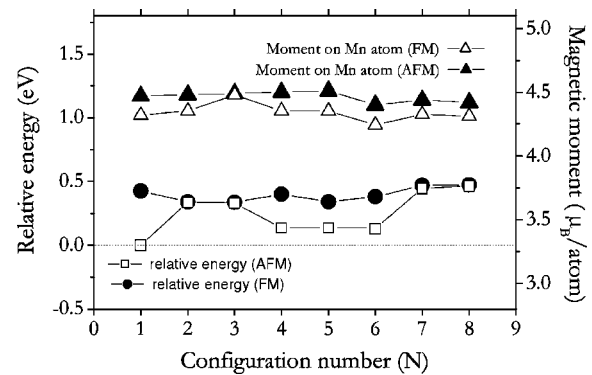

FIG. 3. Magnetic moments and relative energies calculated with respect to the antiferromagnetic ground state in Mn-doped ZnO thin film corresponding to antiferromagnetic (AFM) and ferromagnetic (FM) states for different configurations of Mn in $Zn_{28}Mn_4O_{32}$ supercell.

discussed in the above. These energy differences are measured with respect to the ground-state configuration 1 which is antiferromagnetic. Note that the ferromagnetic state in configuration 1 lies 0.11 eV/Mn atom above the antiferromagnetic ground state. This result is consistent with the experiments of Ueda *et al.*,[12] Fukumura *et al.*,[17] Yoon *et al.*,[29] and Kolesnik *et al.*[30] who found (Zn, Mn)O system is antiferromagnetic. While the antiferromagnetic state is consistently lower in energy than the ferromagnetic state, we find that the energy difference $\Delta\varepsilon$ between these states decreases as the distance between Mn atoms increases with the only exception of configuration 5, where the two Mn atoms belong to two different layers. For example, we recall that when Mn atoms form nearest neighbor on the surface layer, they are 3.25 Å apart and $\Delta\varepsilon=-0.11$ eV/Mn atom. On the other hand, when the distance between them is 5.21 and 6.14 Å, $\Delta\varepsilon$ is 0.007 and 0.003 eV/Mn atom, respectively. Thus in the dilute limit when Mn atoms are far apart, the system will display paramagnetic (or spin glass) behavior since there is no preferential direction for the spin to align. This agrees with the experiment of Cheng and Chien.[6] Sato and Katayama-Yoshida[31] have studied the magnetic properties of transition-metal-doped II-VI and III-V bulk semiconductors systematically using the KKR-CPA method and local density approximation. They have found the spin glass state to be the energetically favorable state in the (Zn, Mn)O system.

On the other hand, as concentration increases, Mn atoms can come close to each other, cluster around the O atom, and exhibit antiferromagnetic behavior as seen experimentally.[17,29] Due to this clustering, it can be expected that a secondary phase might appear in some experimental conditions. Recall that a similar process also exists in the Mn-doped GaN system. It was shown recently[32] that clustering of Mn around N is energetically favorable and in small clusters the resulting ferromagnetic coupling between Mn atoms leads to giant magnetic moments. The authors[32] also suggested that the observed ferromagnetism in (Ga, Mn)N with large Curie point could result from this clustering. In a recent experiment, Dhar *et al.*[33] have demonstrated that the origin of the frequently observed high temperature ferromag-

netism in (Ga, Mn)N layers is indeed related to the formation of Mn-rich clusters.

Due to the antiferromagnetic coupling, the (Zn, Mn)O system has no net magnetic moment, as shown in the total density of states (DOS) in Fig. 2(b). The Fermi energy lies in the gap which is considerably reduced from that in pure ZnO [see Fig. 2(a)]. It is found that each Mn atom individually has a magnetic moment of about 4.4 μ_B with opposite spin orientation, and the main contribution comes from the Mn -3d orbital. Figure 2(c) shows the partial DOS for one Mn atom. The hybridization between O-2p and Mn-3d reduces the magnetic moment as compared to that of a free Mn atom. This is different from the case of a MnO dimer,[34] where the $4s^2$ electron of Mn can strongly hybridize with the $2p^4$ electrons of O, thus leaving the $3d^5$ electrons to carry a magnetic moment of $5\mu_B$. However, when Mn atoms are doped substitutionally in ZnO film, in addition to the other surrounding Mn atoms, there are four oxygen atoms bonded to it. The large coordination of oxygen enhances the hybridization among the orbitals, and the magnetic moment is reduced accordingly.

In Fig. 3, we also plot the magnetic moments of the antiferromagnetic (AFM) and ferromagnetic (FM) states for all eight configurations. The magnetic moments localized at the Mn sites in the antiferromagnetic state are slightly larger than those in the ferromagnetic state. A small amount of magnetic moment ($0.14\mu_B$) exists on the O atom. This indicates that the amount of charge transfer from Mn to O is independent of Mn location and that Mn remains as a Mn^{2+} ion. According to the pd Zener model, the ferromagnetism is mediated by holes as in Mn-doped GaAs.[1,2] Since in Mn-doped ZnO, Mn is isoelectronic with Zn, there are no holes to mediate ferromagnetism. This is the physical reason why we find the ground state of $Mn_xZn_{1-x}O$ to be antiferromagnetic. The origin of the observed ferromagnetism in Mn-doped Zn systems in certain experiments[4] remains an unresolved issue.

[1] H. Ohno, Science **281**, 951 (1998).

[2] T. Dietl, H. Ohno, F. Matsukura, J. Cibert, and D. Ferrant, Science **287**, 1019 (2000); H. Ohno, D. Chiba, F. Matsukura, T. Omiya, E. Abe, T. Dietl, Y. Ohno, and K. Ohtani, Nature (London) **408**, 944 (2000).

[3] M. E. Overberg, C. R. Abernachy, and S. J. Pearton, Appl. Phys. Lett. **79**, 1312 (2001); N. Theodoropoulou and A. F. Hebard, *ibid.* **78**, 3475 (2001); M. L. Reed, N. A. EI-Masary, H. H. Stadelmaier, M. K. Ritums, and M. J. Read, *ibid.* **79**, 3473 (2001).

[4] S. W. Jung, S.-J. An, and Gyu-Chul Yi, Appl. Phys. Lett. **80**, 4561 (2002); P. Sharma *et al.*, Nat. Mater. **2**, 673 (2003).

[5] K. V. Rao (private communication).

[6] X. M. Cheng and C. L. Chien, J. Appl. Phys. **93**, 7876 (2003).

[7] K. Hummer, Phys. Status Solidi B **56**, 249 (1973).

[8] Z. Jin, M. Murakami, T. Fukumura, Y. Matsumoto, A. Ohtomo, M. Kawasaki, and H. Koinuma, J. Cryst. Growth **214/215**, 55 (2000).

[9] T. Fukumura, Zhengwu Jin, A. Ohtomo, H. Koinuma, and M. Kawasaki, Appl. Phys. Lett. **75**, 3366 (1999).

[10] Z. Jin, Y.-Z. Yoo, T. Sekiguchi, T. Chikyow, H. Ofuchi, H. Fujioka, M. Oshima, and H. Koinuma, Appl. Phys. Lett. **83**, 39 (2003).

[11] Z. Jin, T. Fukumura, M. Kawasaki, K. Ando, H. Saito, T. Sekiguchi, Y. Z. Yoo, M. Murakami, Y. Matsumoto, T. Hasegawa, and H. Koinuma, Appl. Phys. Lett. **78**, 3824 (2001).

[12] K. Ueda, H. Tabata, and Tomoji Kawai, Appl. Phys. Lett. **79**, 988 (2001).

[13] H. Matsui, H. Saeki, H. Tabata, and T. Kawai, J. Electrochem. Soc. **150**, G508 (2003).

[14] K. Kim, Hyun-Sik Kim, Dae-Kue Hwang, Jae-Hong Lim, and Seong-Ju Parka, Appl. Phys. Lett. **83**, 63 (2003).

[15] X. T. Zhang, Y. C. Liub, J. Y. Zhang, Y. M. Lu, D. Z. Shen, X. W. Fan, and X. G. Kong, J. Cryst. Growth **254**, 80 (2003).

[16] K. Ando, H. Saito, Z. Jin, T. Fukumura, M. Kawasaki, Y. Matsumoto, and H. Koinum, J. Appl. Phys. **89**, 7284 (2001).

[17] T. Fukumura, Z. Jin, M. Kawasaki, T. Shono, T. Hasegawa, S. Koshihara, and H. Koinuma, Appl. Phys. Lett. **78**, 958 (2001).

[18] J. P. Perdew and Y. Wang, Phys. Rev. B **45**, 13 244 (1992).

[19] S. K. Nayak, M. Nooijen, and P. Jena, J. Phys. Chem. A **103**, 9853 (1999).

[20] M. B. Knickelbein, Phys. Rev. Lett. **86**, 5255 (2001).

[21] G. L. Gutsev, B. K. Rao, P. Jena, X-B. Wang, and L-S. Wang, Chem. Phys. Lett. **312**, 598 (1999).

[22] P. E. Bloechl, Phys. Rev. B **50**, 17 953 (1994).

[23] G. Kresse and J. Heffner, Phys. Rev. B **54**, 11 169 (1996).

[24] H. J. Monkhorst and J. D. Pack, Phys. Rev. B **13**, 5188 (1976).

[25] A. Wander and N. M. Harrison, Surf. Sci. **457**, L342 (2000).

[26] A. D. Becke, J. Chem. Phys. **98**, 5648 (1993); C. Lee, W. Yang, and R. G. Parr, Phys. Rev. B **37**, 785 (1988).

[27] B. Meyer and D. Marx, Phys. Rev. B **67**, 035403 (2003).

[28] Q. Wang, Q. Sun, and P. Jena (unpublished).

[29] S. W. Yoon, S.-B. Cho, S. C. We, S. Yoon, B. J. Suh, H. K. Song, and Y. J. Shin, J. Appl. Phys. **93**, 7879 (2003).

[30] S. Kolesnik, B. Dabrowski, and J. Mais, J. Supercond. **15**, 251 (2002).

[31] K. Sato and H. Katayama-Yoshida, Semicond. Sci. Technol. **17**, 367 (2002).

[32] B. K. Rao and P. Jena, Phys. Rev. Lett. **89**, 185504 (2002).

[33] S. Dhar, O. Brandt, A. Trampert, L. Däweritz, K. J. Friedland, and K. H. Plong, Appl. Phys. Lett. **82**, 2077 (2003).

[34] G. L. Gustsev, B. K. Rao, and P. Jena, J. Phys. Chem. A **104**, 5374 (2000).